EG UK Theory and Practice of Computer Graphics (2007)
Ik Soo Lim, David Duce (Editors)

Viewing 0.3Tb Heart Simulation Data At Your Desk

I. J. Grimstead[2], S. Kharche[1], H. Zhang[1] and N. J. Avis[2] and D. W. Walker[2]

[1]Computational Biology Group, School of Physics and Astronomy, University of Manchester, Manchester M60 1QD, UK
[2]School of Computer Science, Cardiff University, Queens Buildings, Cardiff CF5 1AA

Abstract

Atrial fibrillation (AF) affects a large section of the aged population, accounting for nearly 1% of total National Health Service (NHS) expenditure. Modelling of this condition to promote further understanding is hence of extreme importance to the NHS. Such modelling takes considerable compute power, producing large datasets; for instance, an 18 million data point model produces 0.3Tb when simulating 3 seconds of heart activity.
Such large datasets are currently batch processed to produce a movie from a preset camera position. What is needed is a means of reducing the data to a more manageable size, where it can be displayed in real-time at the heart modeller's desk for interactive exploration and evaluation.
We present a pilot study where the Resource-Aware Visualization Environment (RAVE) has been adapted to filter AF datasets ready for subsequent interactive visualization on a desktop machine. A high-end visualization workstation was not required to view the 0.3Tb dataset in real-time, where the modeller could manipulate both camera position/orientation and simulated elapsed time at interactive rates. This has enabled visual inspection and related rapid evaluation of AF, as well as supporting intuitive insight.

Categories and Subject Descriptors (according to ACM CCS): I.3.6 [Computer Graphics]: Methodology and Techniques I.3.8 [Computer Graphics]: Applications J.3 [Life and Medical Sciences]: Health

1. Introduction

Atrial fibrillation (AF) is a condition of the upper half of the heart (the atria) when sinus rhythm in the atria is disturbed. This results in the atria being unable to pump blood to the ventricles, leading to hypertrophy and heart failure. AF, in itself, is not a life threatening condition. It is, however, a precursor to more serious cardiac conditions. Clinically AF is generally identified by studying the P-waveforms from several electro-cardiogram (ECG) leads.

AF is the most common sustained arrhythmia which leads to loss in quality of life and further fatal cardiac complications. AF affects a large section of the aged population and accounts for about 1% of the total National Health Service expenditure [LTM06] in the UK alone, with increasing prevalence. It is characterised by an erratic ECG and re-entrant electrical propagations in the atria. AF induces electrical remodelling (AFER) of membrane ionic channels [BZG*99, WKR01] in atrial cells, and inhomogeneous gap junctional remodelling of atrial tissue [JW00].

Simulating human atrial malfunction using computational models gives us useful insights [KZH05, KMG*06] into the underlying ionic and intracellular processes and helps in understanding of electrical behaviour at the tissue level. Analysis of simulation results is usually by computing mathematical measures like ECG, and by accurate visualization of the evolution of membrane potential and other variables (e.g. $[Ca^{2+}]_i$ variable). So far, visualization has been traditionally treated as a post-simulation batch process and is not generally interactive. This is due to High-Performance Computing resource limitations (such as enforced batch processing, or lack of a directly-connected display). Novel techniques of detailed scientific investigation are required for a better and fuller understanding of the large scale data output from the biophysically detailed simulations based on 3D realistic anatomy.

This paper presents simulations that are being carried out on the virtual human atrium, which are then interactively displayed for review using a novel visualization system. We use biophysically detailed 26 variable ordinary differential equation model of the human atrium [CRN98], incorporate that into a realistic 3D anatomical model of a

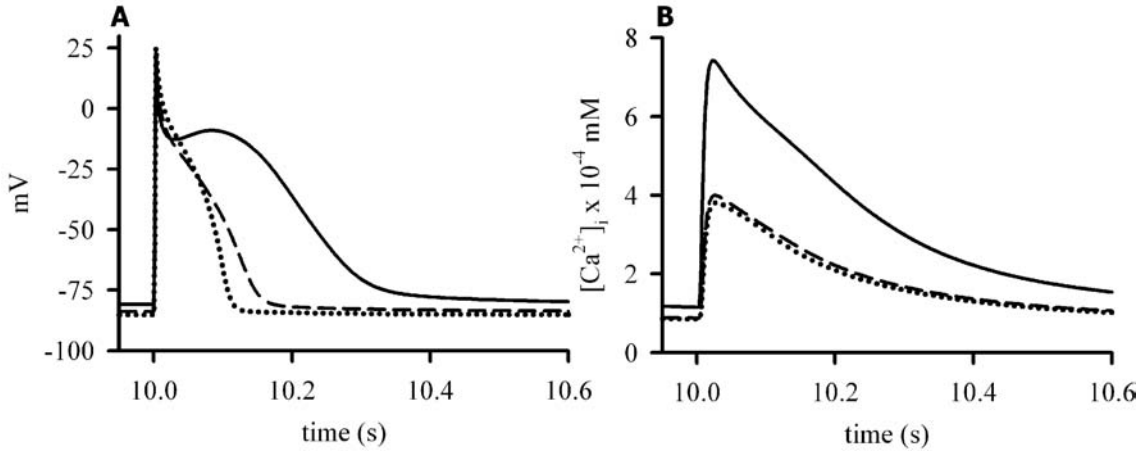

Figure 1: ***A****: Changes in APD. Solid line represents control (normal) data, dashed line represents AF1 data and dotted line AF2 data.* ***B****:* $[Ca^{2+}]_i$ *transients.*

female virtual human atrium [SHB*06] and simulate effects of atrial fibrillation (AF) induced electrical remodelling (AFER) [WKR01,BZG*99] on electrical propagations in the 3D atrium. The large scale data output from the simulations (∼0.3 TB) are processed using RAVE [GAW04] and presented in real-time at the heart modeller's desk. This enabled the modeller to interact with their dataset in a natural manner, without the requirement for local high-end compute.

2. Human Atria Modelling

A biophysically detailed computer model for human atrial cells [CRN98] was used in all simulations. The model was modified to incorporate AFER experimental data on human atrial myocytes [WKR01] (AF1) and [BZG*99] (AF2) to simulate AF remodelling. Among other changes, the main changes due to AF are abbreviation of the electrical excitation (action potential duration (APD)) and a dramatic decrease in calcium ($[Ca^{2+}]_i$) transient amplitude in atrial myocytes. This is shown in Figure 1.

For simulation of electrical propagation in the 3D model, we incorporated the cell models into tissue models using a following parabolic partial differential equation (Equation 1).

$$C_m \frac{\partial u}{\partial t} = D\nabla^2 u - I_{ion} \qquad (1)$$

C_m is cell membrane capacitance, D is the electrotonic diffusion coupling between cells simulating the gap junctional coupling, u is the membrane potential, and I_{ion} is the membrane current. The value of D was taken to be 0.03125 mm2/ms to give a conduction velocity (CV) of 0.27 mm/ms for a solitary wave in control conditions [BBH05]. The 3D anatomically detailed geometry of human female atria was obtained from [SHB*06]. It consists of left atrium (LA), right atrium (RA), pectinate muscles, Bachmann bundle, and sinus node. Spatial resolution in the 3D anatomical model is 0.33 mm × 0.33 mm × 0.33 mm.

Scroll wave re-entry in the 3D homogenous model was initiated in the largest contiguous surface of the right atrium using a cross-field protocol. Electrical activity of 3s was simulated in each case.

Integration in time and space was carried out using an explicit Euler forward time step method while using central differences for spatial derivatives. The integration time step was taken to be 0.005 ms in the cell models. In the 3D simulations, a time step of 0.05 ms was seen to give solutions similar to the smaller time step of 0.005 ms as the space step was 0.33 mm.

3. Supporting Human Atrial Models in RAVE

The Resource-Aware Visualization Environment (RAVE) is used for distributing datasets for collaborative visualization; it can present images using a local graphics processing unit (GPU), or utilise a remote service's GPU to perform the rendering instead. Detail about RAVE's architecture appear elsewhere [GAW04], but we present a brief overview of the system in the next section.

3.1. Resource-Aware Visualization Environment

As shown in Figure 2, at its centre of RAVE is the *data service*, which manages access to the data to be visualised by the user. The RAVE client application initially discovers available data services from a Universal Description, Discovery and Integration (UDDI) [OAS02] server and then se-

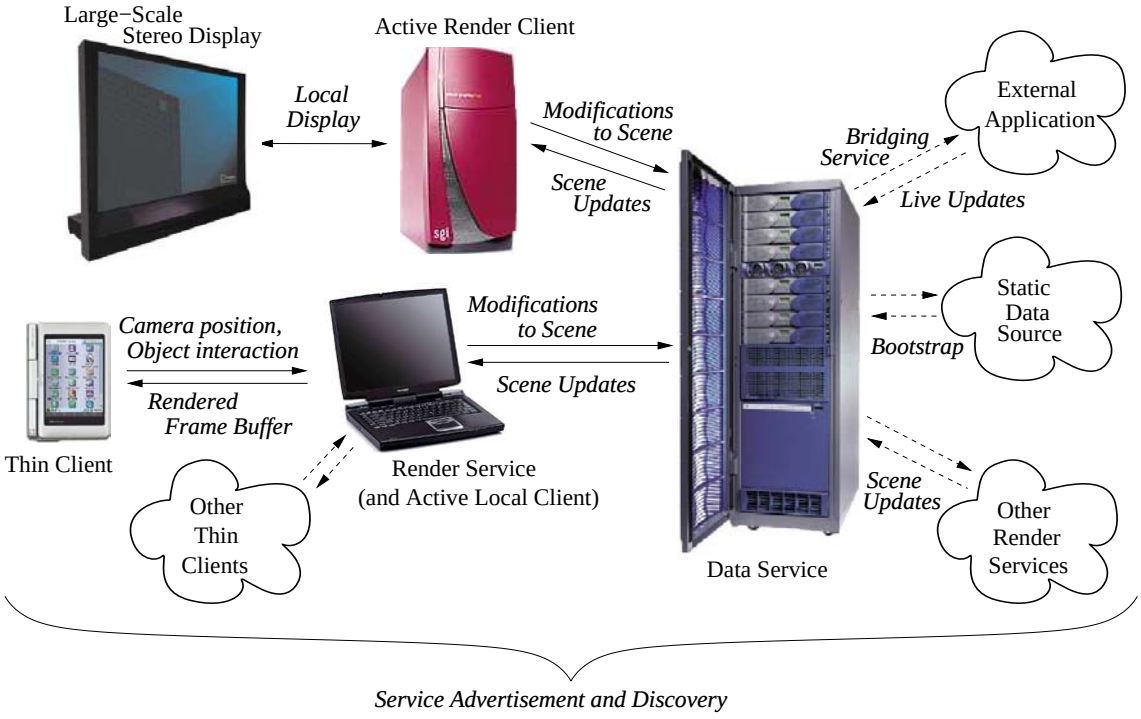

Figure 2: *Architecture of RAVE*

lects the most appropriate service with respect to available resources (such as server memory or network bandwidth). The data service first imports the data set, either from a file (local or hosted on a remote web page) or from a live feed in an external program. The data is then distributed directly to *active clients*, where user's machines have GPUs and are capable of hosting the data set, or instead first sent to a *render server*. The render server renders the data in a similar manner to an active client, only it renders off-screen so as to not disturb the user of the machine hosting the render service. The resulting images are then streamed a s a movie to a *thin client*, which has insufficient local resources to directly store and render the data.

As the rendered scene changes—for example, when the user changes viewpoint or moves an object in the scene—the active client or render server hosting the change transmits this modification back to the data service, which then relays it to the other connected render services and active clients (in effect, implementing a "shared scene graph"). To reduce network traffic, all RAVE clients and services communicate only the changes rather than the entire scene.

RAVE is based on Web service technologies; typically, the data and render services are hosted on different machines, so a client can visualise the data set anywhere on the Internet. However, RAVE is extremely modular and is also layered to hide underlying implementations (such as Web Services, network architecture, etc.). This has enabled a rapid prototype to be created for the pilot study presented in this paper, which only utilised a single, stand-alone active client; data and render services were not used. The feasibility of hosting and interacting such large datasets is our initial goal; once we have achieved this, we will then introduce the support into the remaining parts of the RAVE architecture.

3.2. Storing Human Atrial Models

The RAVE system doesn't require any special software or hardware. It supports various types of data, such as voxels, point clouds, line strips and polygons. RAVE has previously been used to host physiological specimens in point cloud form [GWA*ed], but is further extended to support the much larger temporal simulation data presented here.

The human atrial models consist of over one thousand temporal snapshots of a voxel-encoded region of space, which contains the human atrial model. Each dataset contains approximately 18 million voxels, where each voxel contains two 8-byte doubles, storing voltage and ion strength for $[Ca^{2+}]_i$ (both scalar fields). This results in over 360GB of data, but compresses well (to $\sim$26GB) due to the number of empty voxels in the dataset. However, this is still too large for most machines to store, let alone process in real-time.

Our first stage was for RAVE to pre-process the data by

using threshold values requested by the heart modeller; this revealed the atrial tissue areas inside the volume. As the simulation does not consider movement of the heart, the model is static. Hence position of atrial voxels are unchanging for each temporal snapshot, and can be reused. The thresholding reduced a single frame of the dataset from 18 million voxels down to ∼1.5 million.

However, 1.5 million voxels are still too many to render in real-time, and would require approximately 28GB of memory to store the entire dataset in its current form. Given that the user cannot see inside the heart wall, and the area of interest is the surface of the atrium, we now remove the hidden, internal portions of the atrium (akin to the shell rendering technique [UO93]). This reduction has resulted in a set of 0.6 million voxels.

This reduction was still not enough, as there were over one thousand instances of the dataset as it varied over time; this resulted in approximately 700 million voxels to store and render, or 11.2GB of raw data. The range of voxel values to be visualised was known in advance (from threshold values requested by the heart modeller); a relatively small range of shades of colour would be more than sufficient to observe the results of the simulation. Hence a range of 256 values was selected, as the end user would not be able to discern finer values; this removed the need for a more complex approach, such as direct compression of floating point values [LI06].

The voxel values were mapped from the 64-bit double value to an eight-bit intensity value (one for each of the two datasets), resulting in 16 bits per voxel from the original 128 bits per voxel (one 64-bit double for each dataset). The 8-bit value was then mapped at run-time to a colour for visualization purposes; a simple map to hue (in HSV colour space) was used, mapping low..medium..high values to blue..green..red (as shown later in Section 4.2).

The total data size was now 1.4Gb; this is now approaching the size supported by a modern workstation. However, we still wished to reduce the dataset, to support later work aimed at network transmission. Given that large portions of the dataset may be static for several time instances, we opted for run-length encoding. However, it was discovered that there were very slight fluctuations in value that prevented a strict match from working. These fluctuations were not actually visible to the eye, so we decided to move to lossy run-length encoding, whereby if an intensity value was within 0.5% of the start value, we would regard it as matching. We could increase this threshold as desired, but 0.5% was found to produce sufficient compression without visually affecting the rendered result.

At this point, to simplify rendering and encoding of the dataset, we changed the storage format from a sparse voxel space to individual points (point cloud). This enabled us to use the hardware accelerated rendering support for point clouds in RAVE, and to store the compressed voxel data away from the mapped geometry. Compressed voxel datasets were not supported in hardware by our underlying rendering library (currently Java3D). The selection of point clouds also enabled the pre-calculation of surface normals for correct lighting, which are stored with the points. This finally reduced the underlying data into ∼190MB of data (this shrinks to ∼112MB with gzip, comparing well against 1.4GB without lossy compression) for real-time rendering. This has enabled the rendering of the data on a workstation in real-time using an unstructured point cloud, whilst producing a dataset sufficiently small to transmit over a network.

To interact with this dataset, RAVE has been extended to support temporal data. A new slider bar has been added into the GUI, along with “play”, “stop” and data representation buttons (as can be seen in the bottom of the GUIs in Figures 3-4). The radio buttons enable the user to switch between displayed variables (APD or $[Ca^{2+}]_i$). During playback (or pausing, or random-access frame selection via the slider) of the dataset, full real-time interaction is retained, so the user can rapidly switch between viewed datasets, fly around the scene or move the heart atrium model.

4. Results

We now discuss the results of the simulation in the next section, with analysis of the subsequent visualization in the following section.

4.1. Heart Modelling Output

Simulations were carried out on (i) Sun-Fire 880 UltraSPARC 24 CPUs shared memory system, and (ii) Bull Itanium2 208 CPUs distributed memory system with a single rail Quadrics QsNetII interconnect. The 3D simulations were carried out using parallel OpenMP and MPI solvers developed in our laboratory in Manchester.

AFER produced a remarkable APD abbreviation and reduction in $[Ca^{2+}]_i$ transient amplitude. The APD was reduced by 52.8% (147.6 ms) in AF1 and 65.3% (108.5 ms) as compared to an APD of 313.0 ms in control case. Such APD reduction was consistent with experimental observation [BZG*99, WKR01]. The reduction in APD is reflected in the smaller wavelength of the electrical propagation in the 3D model. Such a reduction in APD is a definite indicator of sustained arrhythmias in atrial tissue.

In the 3D simulations, re-entrant scroll waves were induced on the largest contiguous surface of the RA. This offered the largest substrate for scroll wave initiation and study of their eventual meander. Re-entrant scroll waves have been observed in several systems that can be described using reaction-diffusion. In cardiac excitation, scroll waves occur when electrical sinus rhythm is disturbed, and the electrical propagations follow circular patterns. This leads to rapid excitation of the tissue.

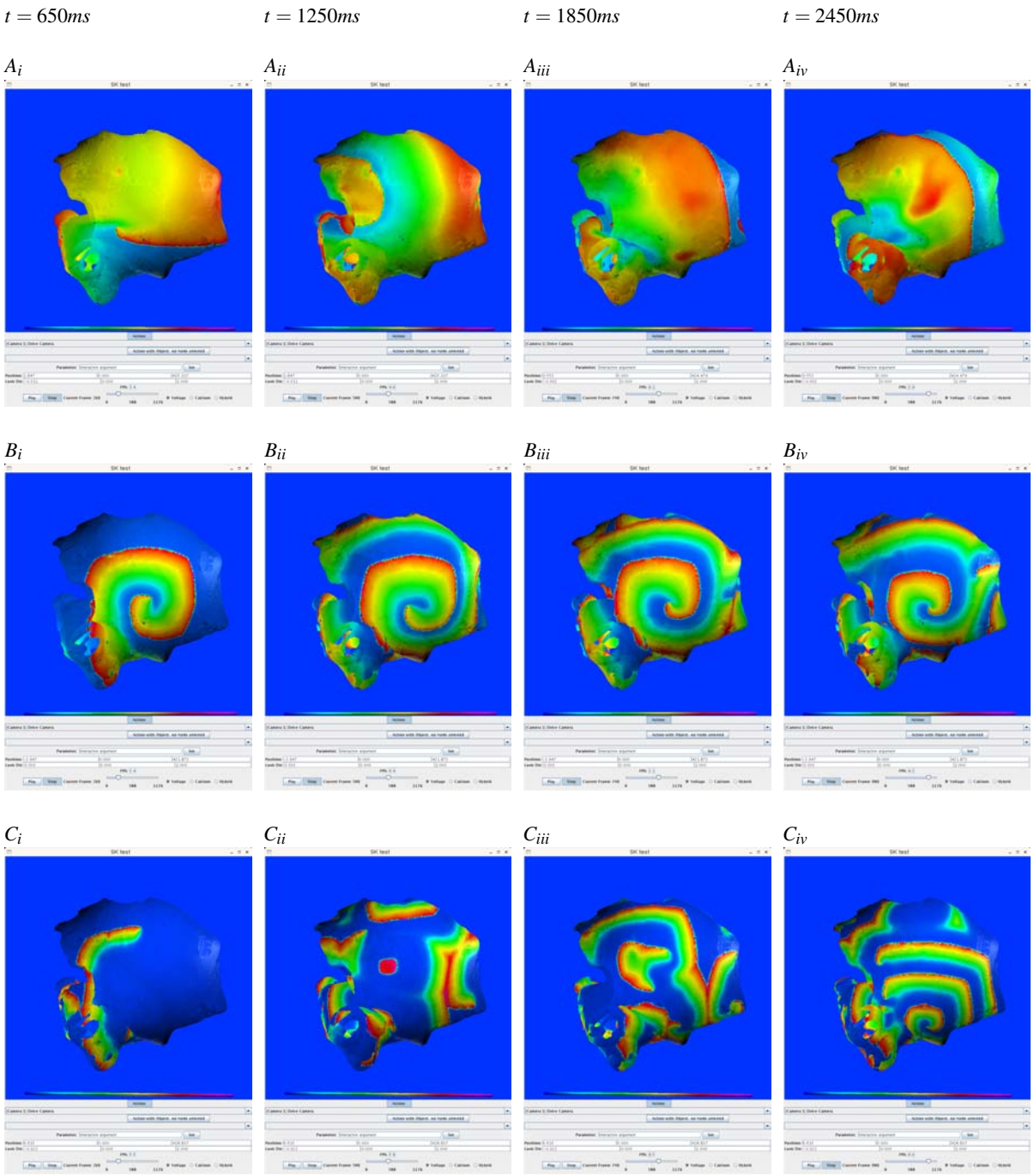

Figure 3: *Scroll waves in the 3D model. Panels A_i, A_{ii}, A_{iii}, A_{iv} show frames from control simulation, B_i, B_{ii}, B_{iii} and B_{iv} show frames from AF1, and C_i, C_{ii}, C_{iii} and C_{iv} show frames from AF2.*

Figure 3 shows the evolution of scroll waves in the three cases. In the control case, the scroll wave quickly meanders away from the point of initiation (∼350 ms after initiation). The meandering scroll waves generally self-terminate. However, in the AF cases, the scroll wave became stable and meandered in a very small region leading to a sustained reentrant excitation driven by mother rotor with indefinite lifespan (lifespan >3000 ms of simulation duration). In addition, in the AF2 case, the scroll wave quickly degenerated into smaller wavelets. These wavelets continued to sustain erratic electrical activity throughout the atrium.

Due to the rapid and erratic electrical activity in the atrium (e.g. AF2), there is loss in mechanical function. In consequence, the atrium is unable to pump blood to the ventricles. During AF, the patient feels pain in the cardiac region for prolonged periods. The patient also has feeling of dizziness and suffers from abnormal blood pressure levels.

Scroll waves, or paroxysmal AF occurs due to temporary disturbance in ionic or structural properties of the atrium. Such AF can become persistent under certain conditions and gives rise to mother rotors. These mother rotors have a small meandering filament, and persist for a long time (usually several months). Mother rotors are known to sustain and feed smaller re-entrant circuits in the atrium.

A mother rotor was seen to emerge after about 2100 ms in AF0. Scroll waves tend to become entrapped by anatomical obstacles, and the meandering scroll wave could also be stabilised. Such entrapment due to anatomical obstacles was observed in the control case, even as AFER did not affect the primary electrical properties of the propagation. This is shown in Figure 4, where the scroll wave was entrapped to the opening of the superior vena cava (SVC) and became highly localised and persisted throughout the simulation. In this case, while the mother rotor was entrapped by the SVC opening hole, the arm of this scroll wave continued to activate atrial tissue close to the SVC at a high rate. This gave rise to alternans type excitations.

4.2. Graphical Representation

RAVE has enabled the presentation of the simulation data as a 3D model which can be interacted with in real-time, whereas previously the data was too large so heart modellers resorted to off-line generated movies.

The interactive nature of RAVE supports the change of viewpoint for the playback of the results, compared to an off-line rendered movie where the viewpoint can only be changed at creation time. This has enabled the rapid navigation of the dataset and hence speeded up its evaluation. This is especially useful when wishing to follow a scroll wave as it travels around the cardiac geometry, as otherwise a fixed viewpoint movie will hide the wave when it travels around the back of the geometry. This can be seen in Figure 4, showing several images taken from 87ms to 107ms simulation time. The camera position/orientation has been moved by the modeller to select the best view, revealing the scroll wave entrapment beginning at the superior vena cava (also called the thoracic blood vessel ostium) in the left-hand image. The series of images show the scroll wave propagating around the atrium.

Identification and study of fibrillation events like anatomical entrapment of electrical waves was facilitated by RAVE functionality. The high resolution realtime visualisation gained by RAVE assisted in identification of such kind of behaviour in our simulation result.

Using the compression techniques in RAVE, this has enabled the simultaneous viewing of several dynamic variables. This simultaneous investigation gives greater understanding into the evolution of the properties of these electrical propagations. Analysis of these results can be carried out numerically, however visual inspection assists intuitive insight. The ability to review the results interactively (changing viewpoint and/or elapsed time) has produced a valuable investigation tool. The ability to change viewpoint to view hidden detail is especially useful, as this is not possible with movies generated with a static viewpoint, and enables viewing inside the geometry which is not usually possible in physiological animal models. In addition, visual representation of the simulation results enhances communication between visualization experts, heart modellers and clinicians.

It must be noted the additional advantage inferred when using RAVE for visualization; a client no longer has to wait for 26GB to download before being able to process the dataset to produce an alternative view. An interactive model can be produced once ∼112MB have been downloaded; this is now sufficiently small for a modeller to submit data for partners to view interactively from their own desks. However, they will not be able to collaborate (yet) as this is a proof-of-concept without full collaboration support, as discussed later in Section 6.

5. Conclusions

AF causes loss in quality of life and demands intensive clinical, physiological and computational modelling research.

Large scale simulation investigation of AF along several avenues enables us to study pathological excitation propagation in virtual atria, dissect contributions of anatomical heterogeniety, dynamic heterogeniety and effects of AFER. This is cost-effective, time-efficient, reduces physiological experimental error and is highly reproducible. We propose to develop it as a predictive patient specific technology to assist in physiological experiments and clinical trials.

Due to continued development of detailed computer simulations, methods for data analysis that provide real time interaction to cardiac modellers will enhance interpretation. This has been provided by RAVE, enabling the heart mod-

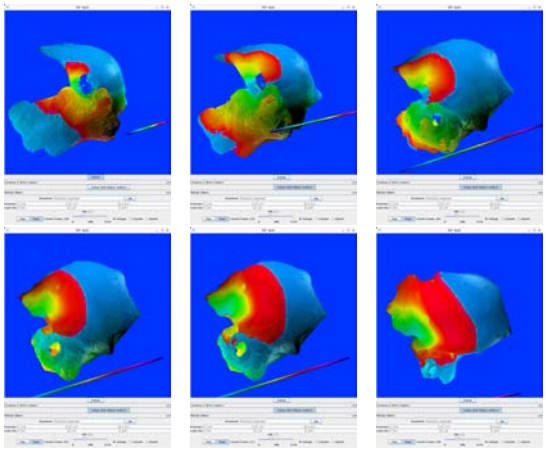

Figure 4: *87ms elapsed: Entrapment begins at superior vena cava location, showing propagation until 107ms elapsed*

ellers to interact with their datasets in real-time without having to use specialist equipment.

6. Future Work

This pilot study has demonstrated the utility of real-time visualization for reviewing simulation results of the virtual human atrium. We now wish to extend this work in RAVE to enable full collaborative support and distributed rendering. This would enable a heart modeller to share their results with colleagues who do not have to download the 0.3TB of data to view the same images, yet still have full interactive access.

We then aim to investigate direct linking of RAVE into the simulation, enabling full computation steering rather than just reviewing the output results. Due to the black-boxing of RAVE and various exposure points to its architecture, computational steering is an achievable goal which may not be possible using other high level visualization software. This would permit the interactive investigation of data, and development of educational tools facilitating demonstration and improving understanding of electrical behaviour in cardiac tissues.

7. Acknowledgements

The work presented here was supported by funding from the British Heart Foundation (PG/06/140), and from VizNET (funded by JISC).

References

[BBH05] BIKTASHEVA I. V., BIKTASHEV V. N., HOLDEN A. V.: Wavebreaks and Self-Termination of Spiral Waves in a Model of Human Atrial Tissue. In *Functional Imaging and Modeling of the Heart* (2005), vol. LNCS 3504, pp. 293–303.

[BZG*99] BOSCH R. F., ZENG X., GRAMMER J. B., POPOVIC C. M., KUHLKAMP V.: Ionic Mechanisms of Electrical Redmodelling in Human Atrial Fibrillation. *Cardiovascular Research 44* (1999), 121–131.

[CRN98] COURTEMANCHE M., RAMIREZ R. J., NATTEL S.: Ionic Mechanisms Underlying Human Atrial Action Potential Properties. *American Journal of Physiology 275* (1998), H301–H321.

[GAW04] GRIMSTEAD I. J., AVIS N. J., WALKER D. W.: Automatic Distribution of Rendering Workloads in a Grid Enabled Collaborative Visualization Environment. In *Proceedings of SC2004: SuperComputing 2004* (November 2004).

[GWA*ed] GRIMSTEAD I. J., WALKER D. W., AVIS N. J., KLEINERMANN F., MCCLURE J.: 3D Anatomical Model Visualization with a Grid-Enabled Environment. *IEEE Computers in Science and Engineering* (accepted).

[JW00] JONGSMA H. J., WILDERS R.: Gap Junctions in Cardiovascular Disease. *Circulation Research 86* (2000), 1193–1197.

[KMG*06] KHARCHE S., MOORE H., GARATT C. J., HANCOX J. C., ZHANG H.: Gain-of-Function in Kir2.1 and its Effects on Atrial Fibrillation in Homogenous Virtual Human Atrial Tissue: A Computer Simulation Study. *Journal of Physiology 3P PC39* (2006).

[KZH05] KHARCHE S., ZHANG H., HOLDEN A. V.: Hypertrophy in Rat Virtual Left Ventricular Cells and Tissue. *LNCS 3504* (2005), 153–161.

[LI06] LINDSTROM P., ISENBURG M.: Fast and efficient compression of floating-point data. *IEEE Trans. Vis. Comput. Graph. 12*, 5 (2006), 1245–1250.

[LTM06] LIP G. Y., TELLO-MONTOLIU H.: Management of Atrial Fibrillation. *Heart 92* (2006), 1177–1182.

[OAS02] OASIS: *Universal Description, Discovery and Integration (UDDI)—Version 2 Specifications*. http://www.oasis-open.org/committees/uddi-spec/doc/tcspecs.htm, July 2002.

[SHB*06] SEEMANN G., HOPER C., B.SACHSE F., DOSSEL O., HOLDEN A. V., ZHANG H.: Heterogeneous Three-Dimensional Anatomical and Electrophysiological Model of Human Atria. *Philosophical Transactions of the Royal Society A, London 364* (2006), 1465–1481.

[UO93] UDUPA J. K., ODHNER D.: Shell rendering. *IEEE Comput. Graph. Appl. 13*, 6 (1993), 58–67.

[WKR01] WORKMAN A. J., KANE K. A., RANKIN A. C.: The Contribution of Ionic Currents to Changes in Refractoriness of Human Atrial Myocytes Associated with Chronic Atrial Fibrillation. *Cardiovascular Research 52* (2001), 226–235.